



Universiteit
Leiden
The Netherlands

Automated planning approaches for non-invasive cardiac valve replacement procedures from CT angiography

Gao, X.; Gao X.

Citation

Gao, X. (2017, November 7). *Automated planning approaches for non-invasive cardiac valve replacement procedures from CT angiography*. *ASCI dissertation series*. Retrieved from <https://hdl.handle.net/1887/57132>

Version: Not Applicable (or Unknown)

License: [Licence agreement concerning inclusion of doctoral thesis in the Institutional Repository of the University of Leiden](#)

Downloaded from: <https://hdl.handle.net/1887/57132>

Note: To cite this publication please use the final published version (if applicable).

Cover Page



Universiteit Leiden



The handle <http://hdl.handle.net/1887/57132> holds various files of this Leiden University dissertation

Author: Gao, Xinpei

Title: Automated planning approaches for non-invasive cardiac valve replacement procedures from CT angiography

Date: 2017-11-07

7

Automated quantification of thoracic aorta dilatation on baseline and follow-up computed tomography angiography

Xinpei Gao, Sara Boccalini, Pieter H. Kitslaar,
Ricardo P.J. Budde, Shengxian Tu,
Boudewijn P.F. Lelieveldt, Jouke Dijkstra, Johan H.C. Reiber.

Abstract

Background Patients with aortic pathologies will undergo lifelong imaging surveillance to determine aortic diameters and their changes over time. According to the guidelines, the measurements of the aorta should be performed at predefined anatomical landmarks and reported accordingly. A framework which can automate the calculation of the changes of the aortic diameters based on multiple scans of the same patient would effectively decrease measurement time and most likely reduce inter-methods and inter-observer variabilities. Notwithstanding, to the best of our knowledge there is no such tool available for thoracic aorta. In this study, we describe and present a validation of an innovative tool for the automatic quantification of thoracic aorta dilatation in baseline and follow-up CTA images.

Methods Patients who underwent two contrast CT scans of the thoracic aorta were included. Diameters of baseline and follow-up scans are automatically generated by the tool, based on multiple landmarks defined on the baseline scans by two operators, were compared with manual measurements performed with the double oblique technique. Bias and correlations were calculated between the methods and, for the automatic framework, between the operators. Bland Altman plots for each location were drawn.

Results Twenty-nine patients were included. The automatic analysis failed in two cases during the centerline extraction and segmentation procedure, which were excluded from further analysis. Our tool showed excellent correlation and small error with the manually generated reference standard, especially for proximal aortic arch (baseline: 0.98, 0.19 ± 1.30 mm; follow up: 0.93, 0.44 ± 2.21 mm), mid descending aorta (baseline: 0.95, 0.37 ± 1.64 mm; follow up: 0.94, 0.37 ± 2.06 mm), and diaphragm (baseline: 0.98, 0.30 ± 1.14 mm; follow up: 0.96, 0.37 ± 1.80 mm). The inter-observer variability was quite low with the errors of the diameters all lower than or around 1mm, and correlations all higher than 0.95. The automatic tool reduced the processing time by half (10-12 minutes auto vs 22 minutes manual).

Conclusion For the first time, a fast and automatic tool was able to derive diameters of baseline and follow-up scans of the thoracic aorta as well as their differences with high accuracy and reproducibility, was presented.

Submitted.

7.1 Introduction

Aortic aneurysms are the second most frequent disease of the aorta after atherosclerosis. The estimated risk of rupture or dissection depends on the maximum diameter of the aneurysm which is also the most important parameter to decide if and when to intervene with surgery or percutaneous intervention (Erbel et al. 2014b; Hiratzka et al. 2010). For patients with aortic dilatation who do not meet the criteria for intervention, imaging follow-up is recommended to monitor diameters at intervals that vary depending also on the underlying aortic pathology. In genetic diseases that affect the aorta, the rate of enlargement progression is higher than in the general population, thus requiring more frequent follow-up. Focal aortic dilatations/aneurysms are a manifestation of a diffuse aortic pathology and therefore the entire aorta, not only the enlarged segment, should be assessed both at baseline and at follow up. To reduce variability between institutions and/or operators, measurements of the aorta should be performed at several specific predefined landmarks and reported accordingly (Erbel et al. 2014b; Goldstein et al. 2015; Hiratzka et al. 2010).

Providing rapid and high resolution images of the entire aorta, CT is the imaging modality of choice to measure aortic diameters both at diagnosis and follow up. Measurements have to be performed in a plane perpendicular to the long axis of the vessel that can be identified manually or by semi-automatic or automatic software (Erbel et al. 2014b). The manual technique requires a workstation for multiplanar reconstructions, knowledge of how to obtain the correct plane of the aortic anatomy as well as the positions of specific landmarks. Moreover for each exam and at all locations, the operator must repeat the process to define the plane perpendicular to the long axis of the aorta ensuing a very time consuming post-processing procedure, especially when the baseline scans have to be reassessed as well. Several commercially available semi-automatic and automatic software are able to detect the aortic centerline and aortic diameters reducing the reporting time and measurement variability especially among non-expert readers (Biesdorf et al. 2012; Entezari et al. 2013; Kauffmann et al. 2011, 2012; Lu et al. 2010). However the reliability of accurate aortic diameter assessment by these published methods has been deemed so low, that previously published thresholds for intervention based on aortic growth over time have been removed from more recent guidelines (Erbel et al. 2014b).

A single framework that would be able to automate the calculation of the differences of aortic diameters from multiple scans of the same patient, would dramatically reduce reporting time and likely improve measurement

reproducibility thereby reducing intermethod, intraobserver and intraobserver variabilities. However, to the best of our knowledge there is no such tool for the thoracic aorta available.

The aim of our study was to analyze the accuracy and reproducibility of our newly developed tool for the automatic assessment of thoracic aorta diameter and the differences over time by comparison with manual measurements.

7.2 Methods

Study population and CT protocol

In this this single-center retrospective study, for which a waiver was received from the local Medical Ethics Committee, two CT scans of patients who had shown an increase of thoracic aorta diameters over time were included. To identify these patients, the PACS of the Erasmus MC was searched for radiological reports of CT scans performed between 2006 and March 2016 and included predefined terms. These terms were: "more dilated", "increase in diameter", "increased dilatation", "wider dilatation", "wider aneurysm", and "change in diameter". Patients with reports containing any of these search phrases were eligible for inclusion regardless of the amount of diameter increase. Next, the quality of the corresponding CT scan and of the one used as a comparison for clinical purposes was subjectively assessed and only patients who two contrast enhanced CT scans with quality had judged acceptable to perfect were included. Whenever the two so identified scans did not have sufficient quality but the patient had undergone prior and/or later scans that met this criterion, the latter were included. In case multiple exams with adequate quality were available, the two with the longest time period in-between were selected. All scans that did not have thin slice reconstructions with angio or soft tissue kernels of the entire thoracic aorta were excluded. Patients with congenital anatomical variations of the aorta were also excluded, with the exception of mild aortic coarctation. All patients who had been operated upon with replacement of any part of the ascending aorta and/or aortic arch prior to the CT scans, were excluded as well. On the other hand, patients operated for aortic coarctation with end-to-end anastomosis or small patches were included.

Patient demographics were retrieved from the electronic patient files. Technical parameters of the CT scans including date, scanner, ECG gating, type of gating, kV, mAs, reconstruction slice thickness, kernel, contrast medium and contrast injection protocol were collected. For the scans performed with ECG-gating also the phase of the cardiac cycle

(approximated at 5% intervals) of the reconstruction employed for manual measurements was noted and whenever possible the same phase was chosen to assess the two scans of a single patient. For prospectively ECG-triggered high-pitch spiral acquisitions the cardiac phase at the level of the aortic valve was considered.

Reference standard

Manual measurements were performed by a radiologist with four years of experience in cardiovascular imaging. For this purpose CT datasets were exported to a multimodality workstation (Syngo.via, Siemens). Measurements were performed on planes perpendicular to the centerline of the aorta that were identified with the double-oblique method by manually rotating the axes. Inner-edge to inner-edge diameters were manually defined.

The maximal diameter was measured. All older scans were assessed first. The more recent scans were assessed at least two weeks after the first ones, by the same radiologist blinded to the results of the first dataset. The time needed to perform all the measurements on one dataset was recorded and the average calculated.

Diameters at different anatomical locations along the aorta

To assess changes of aortic dimensions over time, diameters were measured at multiple and standardized anatomical locations in accordance with the 2014 guidelines of the European Society of Cardiology (ESC) for the diagnosis and treatment of aortic diseases (Erbel et al. 2014b). Diameters were therefore calculated at seven prescribed anatomical locations along the thoracic aorta: sinotubular junction (STJ), mid ascending aorta (MAA), proximal aortic arch (PROX), mid aortic arch, proximal descending thoracic aorta (DIST), mid descending aorta (DESC) and diaphragm. STJ was measured as the connection of the aortic root and the ascending aorta, MAA at the level of the pulmonary trunk, PROX at the origin of the brachiocephalic trunk. The mid aortic arch was located between the left carotid artery and the left subclavian artery; after the left vertebral artery if it had a separate origin from the aorta. DIST was measured at approximately 2 cm distal to the left subclavian artery. However if at this level there was either a dilatation or a steep bending of the aorta, the plane was moved closer to the left subclavian artery. DESC location was placed at the same level as the MAA.

The same landmarks and location were employed for both manual and automatic measurements.

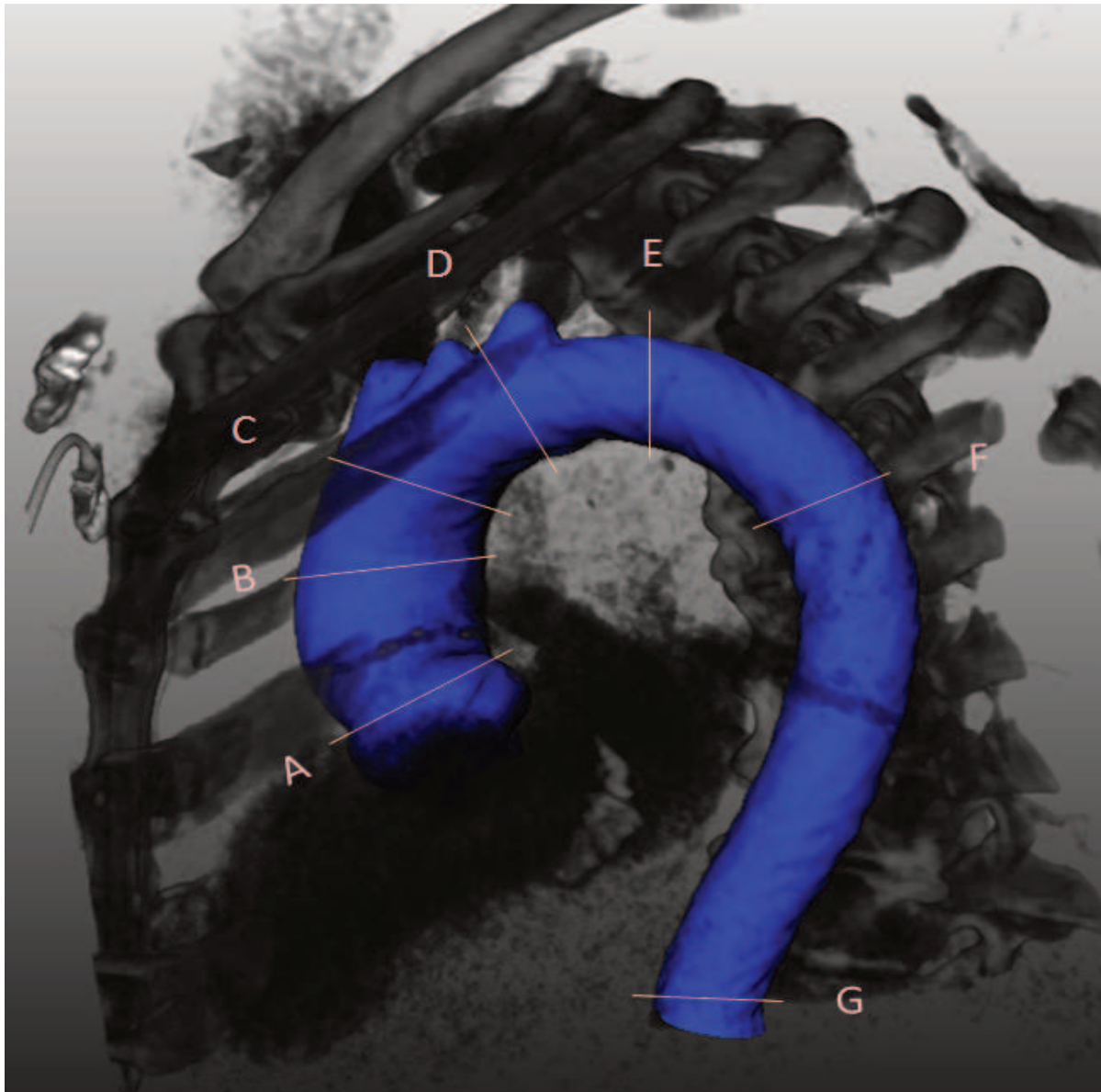


Figure 7.1.3D reconstruction of the thoracic aorta showing the level of the 7 locations where measurements were performed

Automatic aorta dilatation quantification framework

Framework overview

The whole framework was constituted by multiple steps of which the main ones are as follows (Figure 7.2). Firstly the thoracic aorta was segmented from baseline CTA images automatically. In the next step, follow-up images were automatically aligned to baseline image by registration. Subsequently, with the segmented contour of the baseline CTA scan as initial contour, the contour of the thoracic aorta of the follow-up CTA scan was extracted by deforming the initial contour. Finally, based on

the manually defined positions of the seven landmarks along the thoracic aorta on the baseline scan, the maximal diameters of these locations in baseline and follow-up images were calculated.

The automatic framework was implemented in the MeVisLab platform (version 2.7.1, MeVis Medical Solutions AG, Bremen, Germany) using C++ and Python code, and integrated in an in-house tool (AortaDilatationViewer 1.0, LKEB, Leiden, Netherlands).

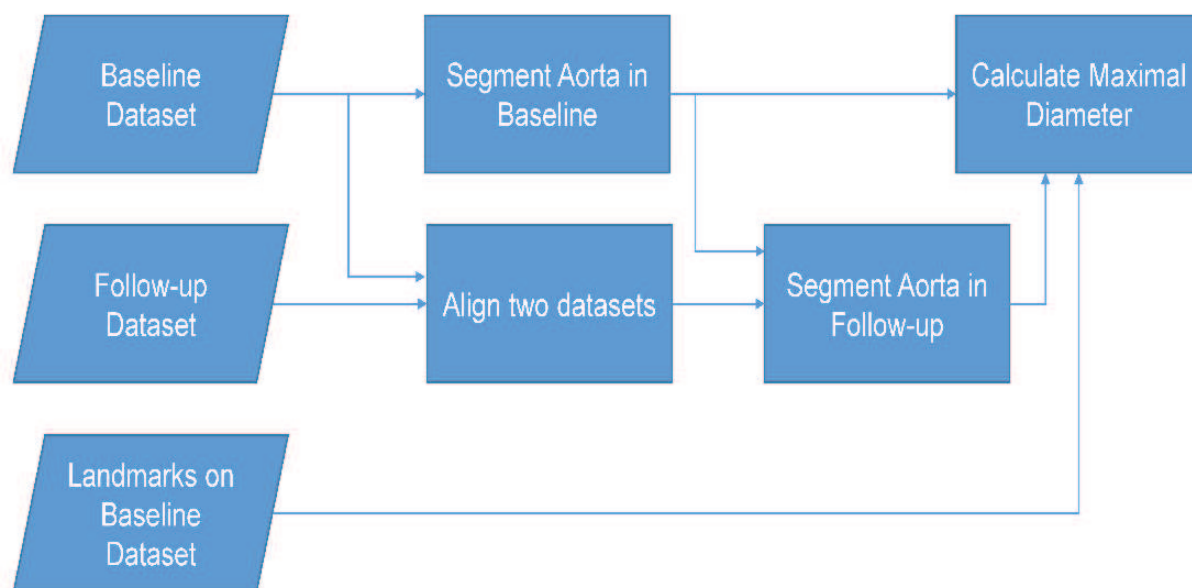


Figure 7.2. Workflow of the automatic aorta dilatation quantification framework

Preprocessing

If the length of the baseline and follow up scans were longer than the region of the thoracic aorta, for instance extended to the femoral arteries, or if the baseline and follow up images had a different length of the aorta that was imaged, datasets were manually adjusted. To minimize the automatic processing of the framework, we manually removed unnecessary images along the z-axis and when the baseline and follow up scans had had a different length of the aorta that was imaged, images from the longer scan were removed until the included anatomical region was the same as in the shorter.

Automatic segmentation of the thoracic aorta of the baseline CTA

The automatic thoracic aorta segmentation scheme in CTA images was based on the centerline extraction and contour detection methods. The centerline extraction method was similar to the algorithm we developed and previously described (Gao et al. 2014), based on wave-propagation algorithm, Gaussian probabilistic distribution model and Dijkstra shortest path algorithm. The previous automatic landmark detection algorithm was

modified from detection of two femoral end points to one aortic end point. The contour detection method was implemented by deformable subdivision surface model fitting algorithm (Kitslaar et al. 2015). In figure 7.2 the result in 3 dimensional grids and 2 dimensional axial views is shown.

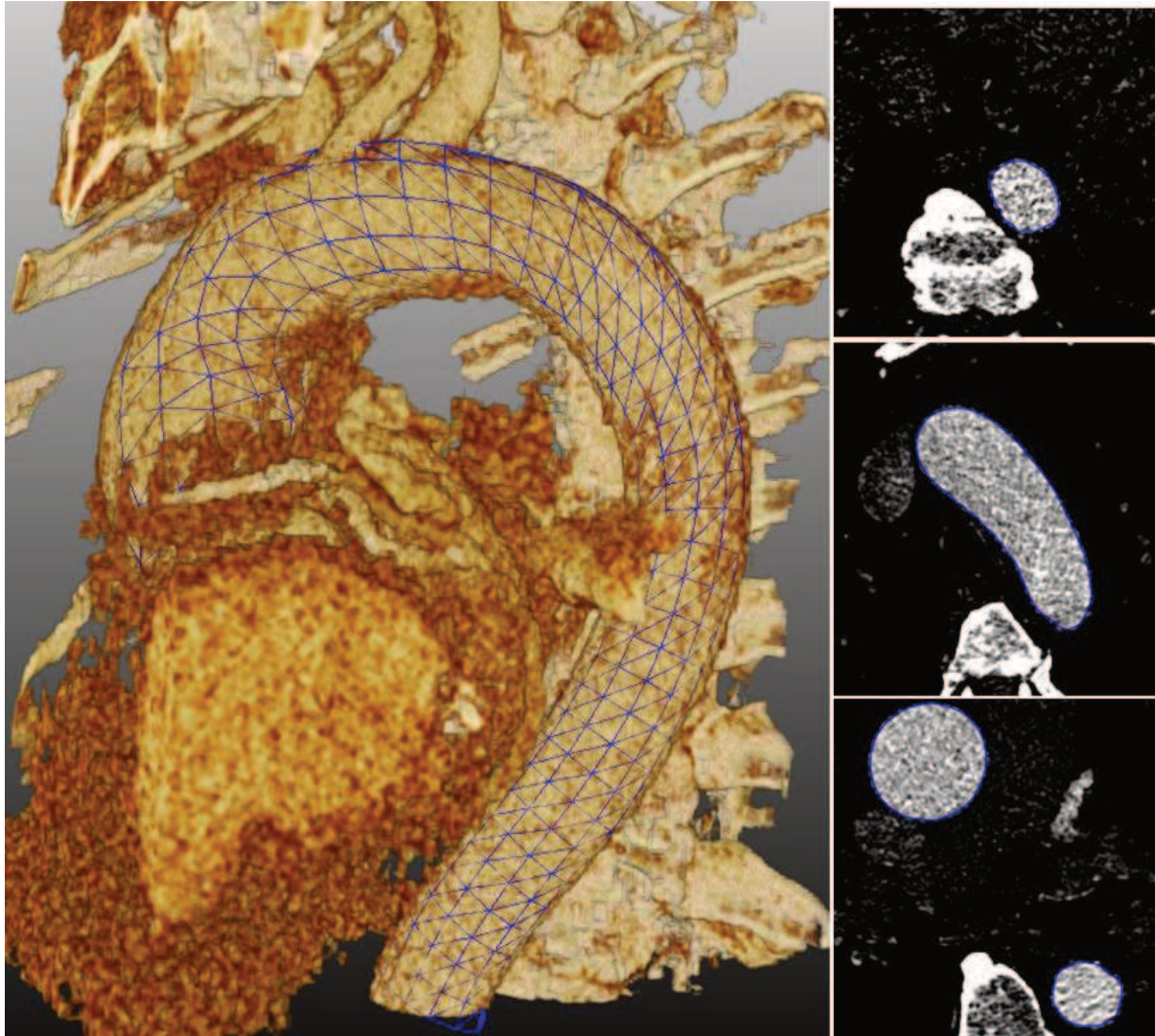


Figure 7.2. 3D grid and 2D axial views showing the result of automatic segmentation

Automatic alignment of baseline and follow up CTA

Automatic alignment was implemented by the registration algorithms. The follow-up image (the moving image) is deformed to fit the baseline image (the fixed image) by registration to find an optimal coordinate transformation. The optimal transformation is obtained while the bias of alignment reaches minimum value. A mask including aorta and surrounding structures was generated by minimum bounding box of the segmented thoracic aorta in the baseline CTA. The mask was used as the mask for the fixed image during registration. The follow-up image was coarsely aligned to the baseline image by rigid transformation at first. Afterwards, affine transformation was implemented for refinement.

Automatic segmentation of the thoracic aorta in follow up CTA

The aligned follow up CTA image was processed by a centerline-based adaptive threshold method (Gao, Kitslaar, Budde, et al. 2016) to reduce the influence of the surrounding tissues in the background, such as high intensity tissue like bone, and low intensity tissue like muscle. With this result image as cost function image and baseline aorta contour as initial contour, the follow-up aorta contour can be obtained by deforming the initial contour according to the intensity of the cost function image. After the segmentation, a region-growing algorithm was used to detect the aortic arch and its branches, in particular at the point of emergence, in detail.

Definition of landmarks for automatic diameter assessment

With the in-house tool, the user could manually annotate the position of the landmarks in multiplanar reconstructions of the baseline scan of each patient. Thereafter the cross-sectional contours of the aorta could be detected by intersecting the landmark plane with the 3D contour, and then the maximum diameter could be calculated automatically. The software automatically identified the same locations and derived the aortic diameter at that level on the follow-up scan.

Visualization of aortic diameters change over time

To improve the visualization of the size change of the aorta, several graphic solutions were implemented in the software and are presented in Figures 7.3 and 7.4.

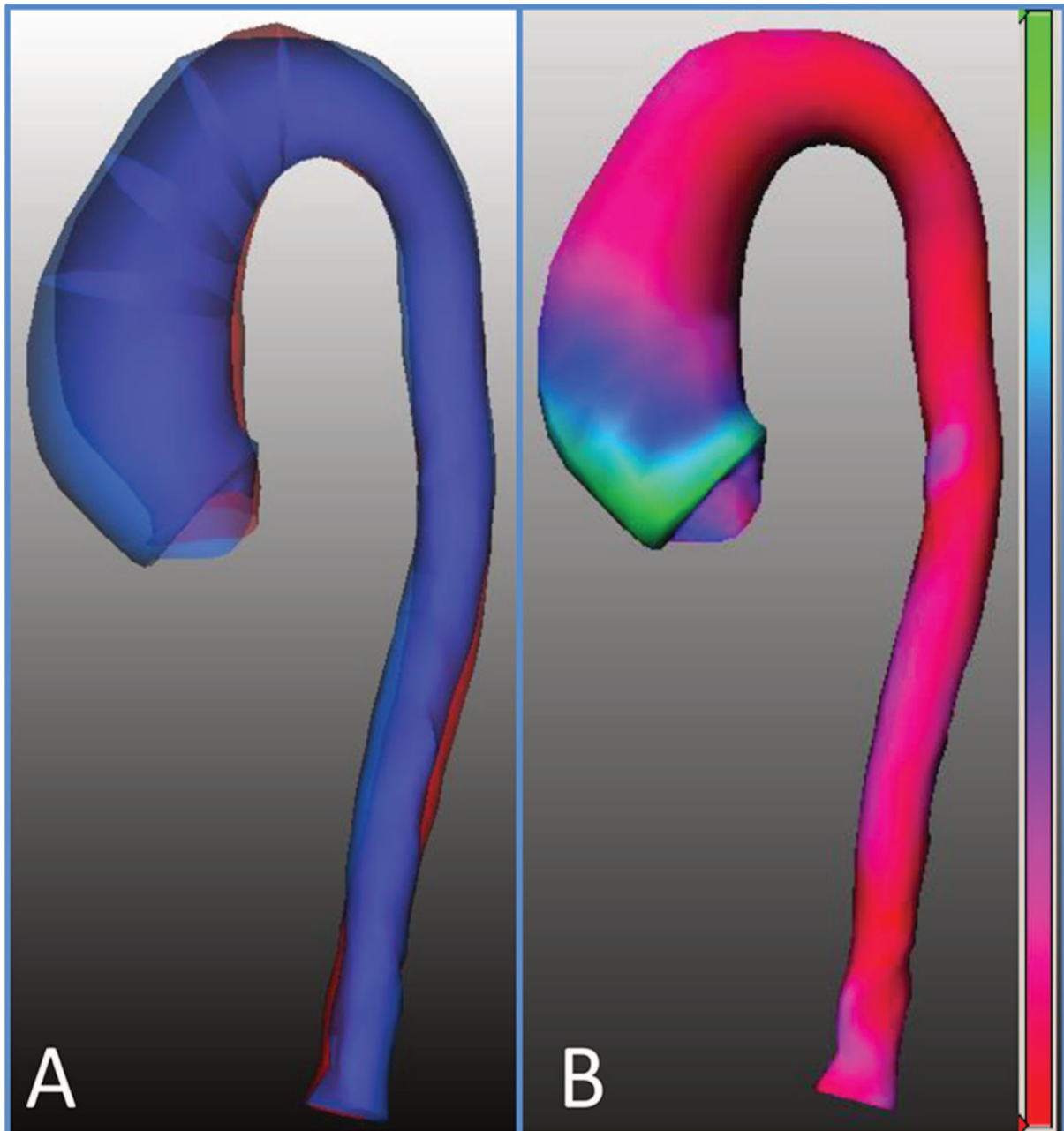


Figure 7.3 Tools for the visualization of the size change of the aorta. In A superimposed 3 dimensional views of the surfaces of the thoracic aorta based on the automatically segmented contour of both baseline (in red) and follow-up (in blue) CTA images. In B the automatically calculated changes in diameters between baseline and follow-up scans are represented with colors (red, blue and green indicate 0, 5 and 10 mm difference in diameters respectively) for an immediate and comprehensive overview of the results.

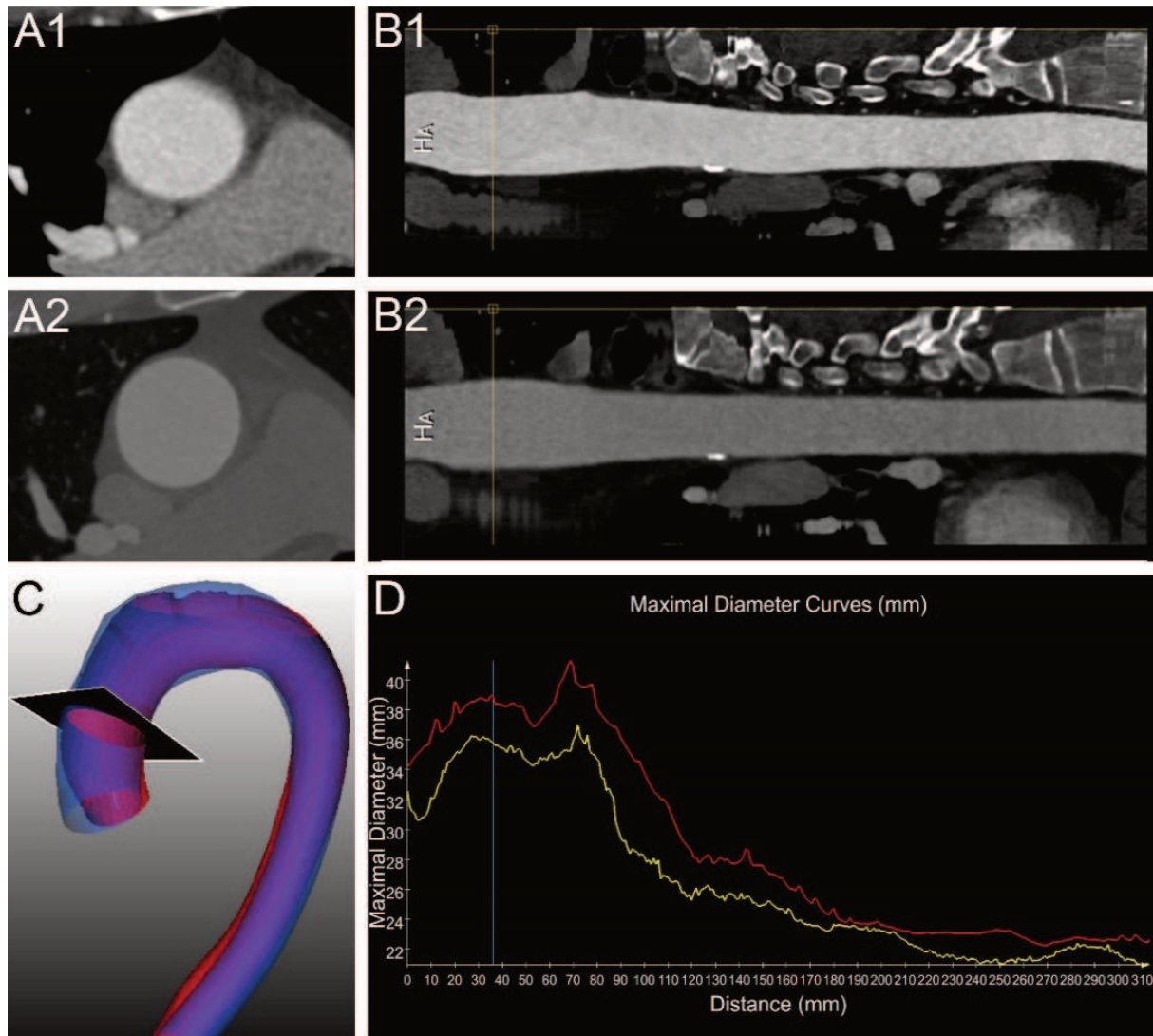


Figure 7.4 Tools for the visualization of the size change of the aorta. Cross-sectional views of the aorta (A1 and A2) and straightened MPR reconstructions (B1 and B2) of the aligned baseline (A1 and B1) and follow-up (A2 and B2) images. In C superimposed 3 dimensional views of the surfaces of the thoracic aorta based on the automatically segmented contour of both baseline (in red) and follow-up (in blue) CTA images. In D the two diameters curves (baseline in yellow and follow-up in red), starting from the sinotubular junction, drawn together on the same graph. The black plane in C shows the level where the cross-sectional diameter indicated by the yellow lines in B1 and B2 and by the blue line in D was calculated.

Inter-observer variability

To analyze the inter-observer variability of the in-house tool, two observers used the in-house tool to annotate the seven aortic landmarks manually on the baseline scan of each patient. Based on these annotations the software automatically generated the following clinical parameters: maximum diameters at the level of the landmarks in baseline and follow-up CTA images, and the progression of the diameters. The inter-observer variability was calculated by comparing the two groups of results. One

observer had 5 years of experience in cardiovascular imaging, the second observer had 4 years of experience.

Statistical analysis

In this study, we used two software SPSS (version 20.0, SPSS Inc., Chicago, IL, USA) and MedCalc (version 15.6, Ostend, Belgium) in the statistical analyses. Quantitative data was analyzed by the mean, standard deviation, and intraclass correlation coefficient (ICC). To visualize the bias between the automatic results from the in-house tool and the reference standard, Bland-Altman plots were drawn. The significance level of the p-value was 0.05.

7.3 Results

Patient population

Twenty-nine patients that had two contrast enhanced CT scans with reasonable to perfect quality of the thoracic aorta were included (23 males; average age $55,5 \pm 14,3$ years). Patient characteristics are summarized in table 7.1.

Four patients had a known congenital aortic disease (2 coarctation and 2 Ehlers-Danlos type 4) and five patients had a bicuspid aortic valve. Six patients had undergone an aortic valve replacement, one a Ross procedure and one an end-to-end anastomosis to correct aortic coarctation.

	Total(n=29)
Male	23(79%)
Age (mean, SD, range) in years	55,5±14,3(25-82)
Height (mean, SD, range) in Kg	1,75±0,1(1,5-1,9)
Weight (mean, SD, range) in m	82,6±18(50-117)
BMI (mean, SD, range)	27,2±6,9(16,9-52,7)
Congenital aortic valve/aortic diseases	
- Ehlers-Danlos 4	2
- BAV	5

- coarctation	2
Risk factors for cardiovascular diseases	
- Smoking	6 (3 past smokers)
- Hypertension	12
- Diabetes	4
- Hypercholesterolemia	8
Previous related surgical procedures	
- Aortic Valve Replacement	6
- Coarctation repair	1
- Ross procedure	1

Table 7.1. Patient population characteristics

CT scans technical parameters

In total 58 scans were included, 29 baseline and 29 follow up examinations. The technical parameters are summarized in Table 7.2. All, but one, scans were acquired with scanners with more than 64 detectors. ECG gating or triggering was employed in most cases (52 scans; =90%). The slice thickness of assessed reconstructions was on average $1 \pm 0,2$ mm and only in two baseline exams the thickness was higher than 1mm.

	Baseline CT scans (=29n)	Follow-up CT scans (=29n)	Total CT scans (=58n)
Patient age at CT (average \pm SD; range) [years]	50,1 \pm 13,7; 22-71	53,4 \pm 14; 24-78	51,7 \pm 13,8
Time difference between CT scans		1187,9 \pm 622,4; 344-2558	

(average \pm SD; range) [days]			
Scanner			
- Sensation 16	1	0	1
- Definition	3	0	8
- Definition AS+	8	0	13
- Definition Flash	12	1	1
- Definition Edge	1	0	1
- Sensation 64	2	1	3
- Somatom Force	2	15	17
kV (average, \pm SD; range) [kV]	106,2 \pm 14,5; 70-120	95,9 \pm 12,9; 70-120	101 \pm 14,6 2
- 70 kV	1	1	8
- 80 kV	2	6	6
- 90 kV	1	5	24
- 100 kV	12	12	2
- 110 kV	0	2	16
- 120 kV	13	3	
Slice thickness (average, \pm SD; range) [mm]	1 \pm 0,2; 0,75-2 2	0,97 \pm 0,1; 0,75-1 3	1 \pm 0,2 5 51
- 0,75 mm	1	26	1
- 1 mm	1	0	1
- 1,5 mm		0	
- 2 mm			
Kernel			
- B20f	9	2	11
- B25f	1	0	1
- B26f	10	1	11
- Bv40	2	15	17
- I26f	6	11	17
ECG-gating			
- not gated	6	0	6
- unknown protocol	1	2	3
- retrospective	2	1	3
- prospective	7	5	12
- prospective high- pitch	12	21	33

Phase of the cardiac cycle			
	2	4	6
- 0%-20%	5	12	17
- 25%-40%	5	9	14
- 45%-60%	11	3	14
- 65%-80%			

Table 7.2. CT scans technical parameters

Success rate of registration and segmentation

Out of the 29 patients, 2 patients were excluded from further analysis. In the first patient, the automatic centerline extraction failed in the baseline image; and in the second patient, the region growing step failed in the baseline image.

Accuracy of the tool

Table 7.3 shows the mean and standard deviation of the maximal cross-sectional diameters at different landmarks by manual measurement and automatic measurements from two observers.

As shown in Table 7.4, for observer 1 the mean differences between the manual measurement and the automatic measurement at different landmarks were all lower than 1mm except at the mid aortic arch, the mid ascending aorta and the sinotubular junction. In the baseline and the follow-up scans, the ICC were all higher than 0.90.

As shown in Table 7.4, also for observer 2 the mean differences at different landmarks were all lower than 1mm except at the mid aortic arch and the sinotubular junction. The ICC coefficients for baseline diameters were all higher than 0.90.

Bland Altman plots for the differences between the two observers and the automatic results combining data from the baseline and follow-up scans for each of the seven locations are shown in Figure 7.5-7.6.

Maximal diameter (mm)	Baseline			Follow up		
	Manu al	Automat ic 1	Automat ic 2	Manu al	Automat ic 1	Automatic 2
Sinotubular junction	37 ± 5	40 ± 5	39 ± 5	39 ± 5	42 ± 5	42 ± 4
Mid ascending aorta	44 ± 5	43 ± 6	44 ± 6	47 ± 6	45 ± 6	46 ± 6
Proximal aortic arch	37 ± 5	37 ± 4	38 ± 5	39 ± 4	39 ± 4	39 ± 4
Mid aortic arch	29 ± 3	30 ± 5	30 ± 5	30 ± 4	33 ± 5	32 ± 5
Proximal descending aorta	27 ± 5	27 ± 5	27 ± 5	29 ± 7	30 ± 6	29 ± 6
Mid descending aorta	26 ± 4	26 ± 4	26 ± 4	27 ± 4	28 ± 5	27 ± 5
Diaphragm	24 ± 4	24 ± 5	24 ± 4	25 ± 4	25 ± 5	25 ± 5

Table 7.3. Average diameter in different locations along the aorta. Manual = measurements performed manually with the double oblique method by observer 1. Automatic 1 and Automatic 2 = automatically calculated diameters based on the locations identified on the baseline scan by observer 1 and 2 respectively. Data as mean ± SD.

Maximal diameter Automatic 1 vs Manual		Sinotubular junction	Mid ascending aorta	Proximal aortic arch	Mid aortic arch	Proximal descending aorta	Mid descending aorta	Diaphragm
Baseline	Mean difference \pm SD [mm]	2.22 \pm 2.19	1.07 \pm 2.20	0.19 \pm 1.30	1.15 \pm 2.33	0.22 \pm 0.97	0.37 \pm 1.64	0.30 \pm 1.14
	ICC	0.95	0.96	0.98	0.91	0.99	0.95	0.98
Follow-up	Mean difference \pm SD [mm]	2.96 \pm 2.64	1.30 \pm 2.45	0.44 \pm 2.21	2.37 \pm 2.59	0.93 \pm 2.79	0.37 \pm 2.06	0.37 \pm 1.80
	ICC	0.92	0.96	0.93	0.90	0.95	0.94	0.96
Maximal diameter Automatic 2 vs Manual		Sinotubular junction	Mid ascending aorta	Proximal aortic arch	Mid aortic arch	Proximal descending aorta	Mid descending aorta	Diaphragm
Baseline	Mean difference \pm SD [mm]	1.96 \pm 1.79	0.44 \pm 1.65	0.56 \pm 1.22	1.19 \pm 1.92	0.00 \pm 1.41	0.37 \pm 2.02	0.41 \pm 1.05
	ICC	0.97	0.97	0.98	0.94	0.98	0.93	0.98
Follow-up	Mean difference \pm SD [mm]	3.15 \pm 2.57	0.26 \pm 2.01	0.85 \pm 2.09	2.26 \pm 2.57	0.59 \pm 2.56	0.04 \pm 2.30	0.30 \pm 1.56
	ICC	0.92	0.97	0.94	0.91	0.96	0.93	0.97

Table 7.4. Assessment of automatic framework compared with manual results. The automatic results were generated based on landmarks defined by observer 1 (Automatic 1) and observer 2 (Automatic 2).

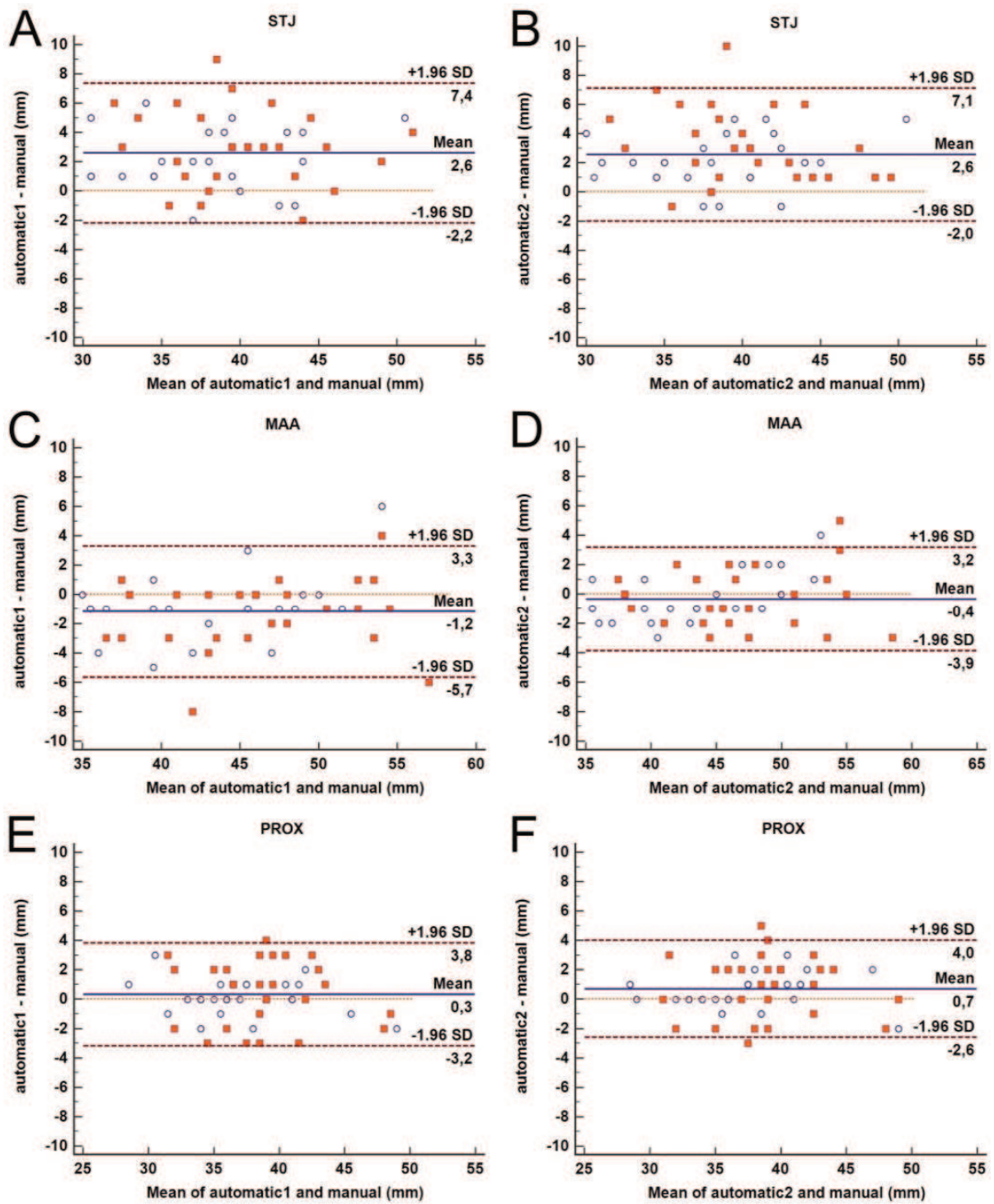


Figure 7.5. Bland-Altman plots representing the difference between automatic and manual measurements at sinotubular junction (A-B), MAA (C-D) and PROX (E-F). Blue circles: baseline diameters. Red squares: follow-up diameters.

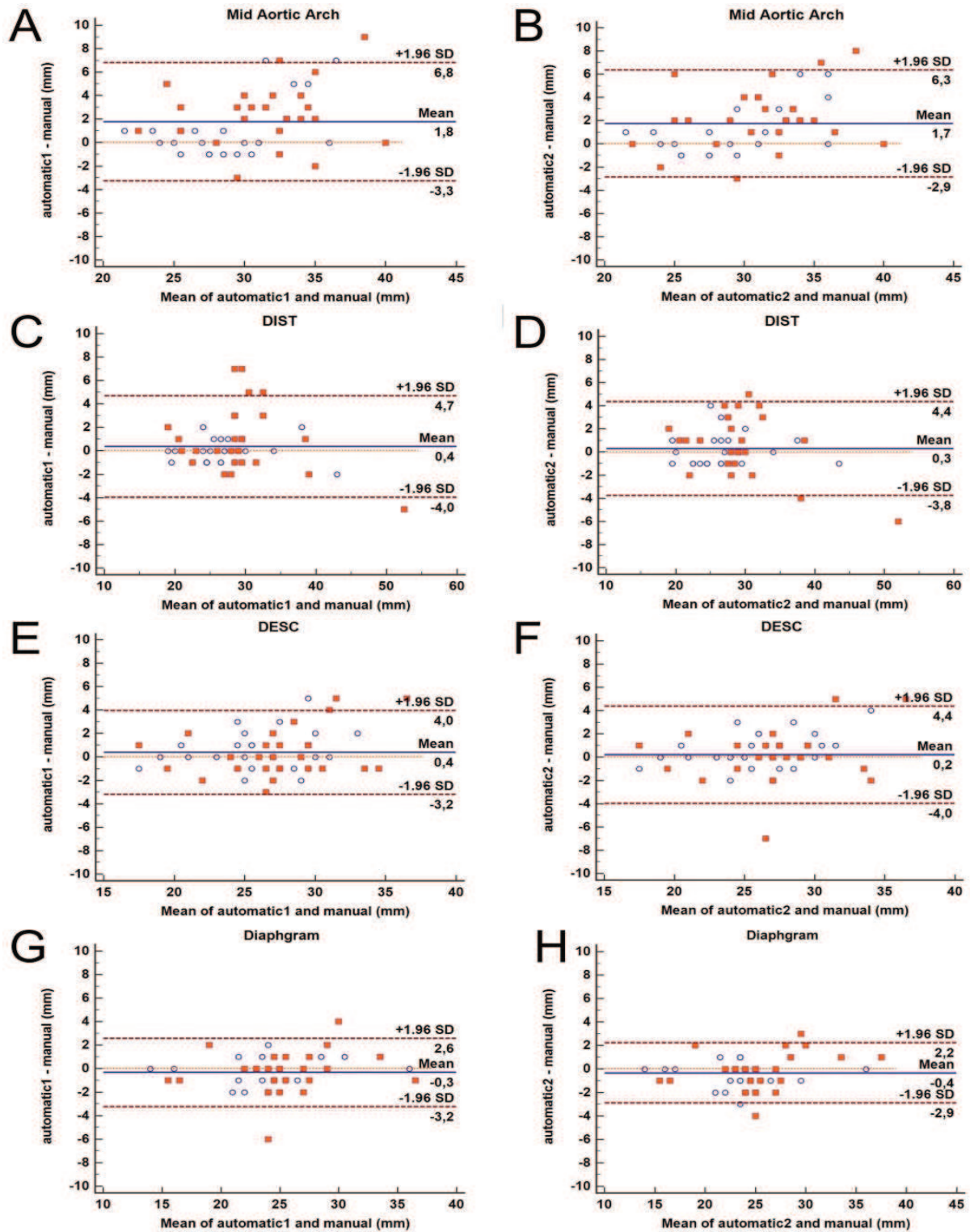


Figure 7.6. Bland-Altman plots representing the difference between automatic and manual measurements at mid aortic arch (A-B), DIST (C-D), DESC (E-F) and diaphragm (G-H). Blue circles: baseline diameters. Red squares: follow-up diameters.

Inter-observer variability

The inter-observer variability of the automatic framework is shown in Table 7.5. The automatic framework showed low inter-observer variability. The mean differences were all lower than 1 mm or around 1 mm at all the landmark locations, and the ICC values all higher than 0.90.

Maximal diameter Automatic 1 vs Automatic 2		Sinotubular junction	Mid ascending aorta	Proximal aortic arch	Mid aortic arch	Proximal descending aorta	Mid descending aorta	Diaphragm
Baseline	Mean difference \pm SD [mm]	0.26 \pm 1.35	0.63 \pm 2.40	0.37 \pm 1.21	0.04 \pm 2.03	0.22 \pm 1.25	0.00 \pm 1.62	0.11 \pm 0.75
	ICC	0.98	0.96	0.98	0.95	0.99	0.96	0.99
Follow-up	Mean difference \pm SD [mm]	0.19 \pm 1.62	1.04 \pm 1.93	0.41 \pm 1.15	0.11 \pm 1.22	0.33 \pm 1.36	0.33 \pm 1.52	0.07 \pm 0.92
	ICC	0.97	0.98	0.98	0.98	0.99	0.97	0.99

Table 7.5. Assessment of automatic framework compared with manual results. The automatic results were generated based on landmarks defined by observer 2.

Time consumption for automatic and manual measurements

The overall mean time to manually measure all the diameters on both baseline and follow up scans was 22.3 minutes (11.4 minutes for baseline, 10.9 minutes for follow up exams). The average time for automatic measurement of both baseline and follow up diameters was about 10 - 12 (4 minutes for landmark annotation, 2 minutes for the automatic processing of baseline images, 6 minutes for the automatic measurement of the follow up images and comparison with baseline).

7.4 Discussion

The natural history of the aorta and aortic aneurysms is to enlarge over time. The rate of (possibly lethal) complications, such as rupture and dissection, increases as the diameter of the aneurysm grows. Therefore these patients will undergo surveillance with imaging techniques at regular intervals until the dilatation has reached a threshold for which it is safer to intervene than to wait and varies depending on the involved aortic segment and underlying aortic pathology (Erbel et al. 2014b). CT is the imaging modality of choice for this purpose. Also the rate of enlargement over time varies depending on the same variables and is estimated to be 0.07 cm/year for the ascending aorta and 0.19 cm/year for the descending aorta in the general population without genetic aortic pathology (Davies et al. 2002). In the 2010 guidelines of the ACCF/AHA/AATS/ACR/ASA/SCA/SCAI/SIR/STS/SVM (Hiratzka et al. 2010) intervention was proposed also before the absolute threshold sizes were reached, as long as a growth rate higher than expected, for instance of more than 0.5 cm/year for aneurysms without an associated genetic aortic pathology, was demonstrated. In the more recent ESC guidelines (Erbel et al. 2014b) growth thresholds have been removed due to the high variability of aortic measurements. To improve accuracy it has been suggested to derive diameters on planes perpendicular to the long axis of the aorta and at predefined and specific landmarks. Although the double-oblique technique has been regarded and used as the reference standard for aortic measurements, it has been associated with intra and interobserver variabilities (defined as mean difference \pm SD) as high as $-0,8\pm 1,3$ mm and $1,3\pm 2$ mm respectively and absolute difference values of up to 11 mm (Quint et al. 2013). It has also been demonstrated that the experience of the observers plays an important role in reducing the variability (Rengier et al. 2009). Therefore notwithstanding standardization of the measurements it is suggested that only differences over time of more than 5 mm should be considered relevant (Erbel et al. 2014a). Moreover, time consumption is an important limitation to the applicability of the double oblique method in daily clinical practice since at all locations and for each exam the axes have to be adjusted to obtain a plane perpendicular to the centerline of the aorta.

Several automatic software packages for aortic measurements have been validated and showed lower intra and interobserver variability and reduced measurement time compared to manual measurements (Biesdorf et al. 2012; Entezari et al. 2013; Kauffmann et al. 2011, 2012; Lu et al. 2010). Only a very limited number of studies described an automated segmentation tool for the thoracic aorta, due to the more complex anatomical structure of the thoracic aorta compared to the abdominal aorta (Biesdorf et al. 2012; Entezari et al. 2013; Lu et al. 2010).

In the study by Biesdorf et al. (Biesdorf et al. 2012) the aortic arch was segmented by three approaches: model-based approach, 2D joint approach and 3D joint approach. The error of the maximal diameter in the ten 3D CTA images with pathologies of the aorta was 2.24 ± 0.72 mm for

the model-based approach, 1.51 ± 0.66 mm for the 2D joint approach, and 1.52 ± 0.69 mm for the 3D joint approach. In the seven 3D CTA images with severe pathologies, the error was 5.45 ± 2.98 mm for the model-based approach, 3.34 ± 2.23 mm for the 2D joint approach, 2.04 ± 0.83 mm for the 3D joint approach. In Lu et al.'s study (Lu et al. 2010) the ascending aorta was semi-automatically measured by two observers to assess the inter-observer variability of the tool. The inter-observer variability was 1.1 mm during the first session of measurements, and 1.2 mm during the second session. However, no comparison against manual reference standard was performed. The tool by Entezari et al. (Entezari et al. 2013) which can segment the thoracic aorta semi-automatically was the one with the most similar features to our study, however it only segmented and measured the thoracic aorta diameters without automatic comparison between two exams of the same patient. The maximum diameters were measured manually and semi-automatically in multiple locations and the mean difference was calculated: all the differences were less than 1mm, except at the sinotubular junction and proximal aortic arch.

Our study not only estimates the accuracy of the automatic diameter measurement tool, but also evaluates the inter-observer variability. For baseline scans all the differences between manual and automatic measurements performed by the two observers were smaller than 1 mm except at the sinotubular junction, mid ascending aorta (only for one observer) and mid aortic arch. The ICC values were all higher than 0.90. The inter-observer variability was less than 1mm with ICC values higher than 0.95 at all locations. The fully automatic contour detection algorithm in our tool for the baseline thoracic aorta has at least similar or even better accuracy and reproducibility compared to the published semi-automatic tools listed above.

To the best of our knowledge, only one study was published presenting a software that allows automatic calculation and comparison of baseline and follow up abdominal aneurysms volume and diameters (Kauffmann et al. 2012). The software described by Kauffman et al. relies on the semi-automatic segmentation of both datasets with the operators' intervention at multiple steps such as the user definition of the aortic lumen location and the correction of aortic contours. In our framework, the segmentation is fully automatic. Kauffman et al.'s study evaluated the inter-observer variability between a senior radiologist and one of three medical students: the mean difference between different observers was 0.07 mm, the ICC values between the senior radiologist and the three medical students for baseline and follow-up examinations were in the range from 0.989 to 0.998. However in this study the performance of the software was not compared to a reference standard. They mentioned that in their previous study (Kauffmann et al. 2011), the accuracy of the software was estimated by comparing the maximal diameter obtained by the semi-automated software to manual measurement, with a mean error of 1.1 ± 0.9 mm. To the best of our knowledge there have been no descriptions of a framework that can automatically align the baseline and follow-up CT datasets of the thoracic

aorta of the same patient and measure the diameters of both scans at the same time.

Compared to the published studies, our framework presents the following new features: 1) The centerline extraction and the contour detection steps in the framework are both fully-automatic without requiring user interaction; 2) The landmark locations can be automatically detected in the follow-up images; 3) The contours of both the baseline and follow up images can be automatically detected and compared; 4) The dilatation of the aorta (difference in diameters) between the baseline and the follow up, can be visualized in color coding on a 3D reconstruction which gives an instantaneous overview of all relevant information; 5) The maximum diameter of the mid aortic arch was quantified automatically for the first time.

For the automatic detection of the follow up thoracic aorta diameters at the level of the landmarks identified on the baseline scan, which has never been implemented in previous studies, the accuracy was evaluated by comparing the maximal diameter at different locations to the manual measurements. For both observers all the differences were smaller than 1 mm except at the sinotubular junction, and mid aortic arch; for one observer they were higher than 1 mm also at mid ascending aorta. The inter-observer variability was less than 1 mm at all locations except at mid ascending aorta (1.04 mm), while the ICC were all higher than 0.95. The accuracy and reproducibility of measurements on follow-up scans of the thoracic aorta proved to be comparable to the results on baseline datasets.

There are some limitations in this study. Firstly, the patient number in this study is relatively small due to the strict inclusion criteria (patients with clinical reports indicating changes in aortic diameters; no congenital aortic anomalies or previous surgery; both baseline and follow-up scans with reasonable to high quality and thin slices reconstructions). Especially the choice to include a priori only scans with reasonable to high quality does not reflect real world variability and further studies are needed to validate the software with a broader spectrum of scans quality. Thirdly, measurements were not compared to a real gold standard. However this is a general issue for studies regarding aortic diameters assessment with imaging techniques since, even if the patients underwent surgery during which aortic dimensions were derived, measurements performed in this setting cannot be considered the gold standard.

7.5 Conclusion

In conclusion, for the first time, an automatic tool which is able to align the baseline and the follow up images to measure the thoracic aorta was developed and evaluated. The tool has high accuracy and reproducibility, especially in the locations PROX, DESC, and diaphragm. The automatic calculation time was half that of the manual measurement time.

